1521-0103/351/3/674–684$25.00
THE JOURNAL OF PHARMACOLOGY AND EXPERIMENTAL THERAPEUTICS

http://dx.doi.org/10.1124/jpet.114.218461
J Pharmacol Exp Ther 351:674–684, December 2014

The Journal of PHARMACOLOGY And Experimental Therapeutics

The Antimalarial Drug Proguanil Is an Antagonist at 5-HT_3 Receptors

Martin Lochner and Andrew J. Thompson

Department of Pharmacology, Cambridge University, Cambridge, United Kingdom (A.J.T.); and Department of Chemistry and Biochemistry, University of Bern, Bern, Switzerland (M.L.)

Received July 28, 2014; accepted October 1, 2014

ABSTRACT

Proguanil is an antimalarial prodrug that is metabolized to 4-chlorophenyl-1-biguanide (CPB) and the active metabolite cycloguanil (CG). These compounds are structurally related to *meta*-chlorophenyl biguanide (*m*CPBG), a 5-hydroxytryptamine 3 (5-HT_3) receptor agonist. Here we examine the effects of proguanil and its metabolites on the electrophysiology and ligand-binding properties of human 5-HT_3A receptors expressed in *Xenopus* oocytes and human embryonic kidney 293 cells, respectively. 5-HT_3 receptor responses were reversibly inhibited by proguanil, with an IC_{50} of 1.81 μM. Competitive antagonism was shown by a lack of voltage-dependence, Schild plot (K_b = 1.70 μM), and radioligand competition (K_i = 2.61 μM) with the 5-HT_3 receptor antagonist [^{3}H]granisetron. Kinetic measurements ($k_{on} = 4.0 \times 10^4$ M^{-1} s^{-1}; k_{off} = 0.23 s^{-1}) were consistent with a simple bimolecular reaction scheme with a K_b of 4.35 μM. The metabolites CG and CPB similarly inhibited 5-HT_3 receptors as assessed by IC_{50} (1.48 and 4.36 μM, respectively), Schild plot (K_b = 2.97 and 11.4 μM), and radioligand competition (K_i = 4.89 and 0.41 μM). At higher concentrations, CPB was a partial agonist (EC_{50} = 14.1 μM; I/I_{max} = 0.013). These results demonstrate that proguanil competitively inhibits 5-HT_3 receptors, with an IC_{50} that exceeds whole-blood concentrations following its oral administration. They may therefore be responsible for the occasional gastrointestinal side effects, nausea, and vomiting reported following its use. Clinical development of related compounds should therefore consider effects at 5-HT_3 receptors as an early indication of possible unwanted gastrointestinal side effects.

Introduction

Proguanil is a prophylactic antimalarial drug that is often taken in combination with other antimalarials, such as atovaquone or chloroquine. In the liver, cytochrome P450 enzymes convert it into 4-chlorophenyl-1-biguanide (CPB) and the active metabolite cycloguanil (CG). Proguanil belongs to the class of phenyl biguanides and has obvious structural similarities to the well known 5-hydroxytryptamine 3 (5-HT_3) receptor agonist *meta*-chlorophenyl biguanide (*m*CPBG). It is therefore possible that proguanil interacts with 5-HT_3 receptors.

5-HT_3 receptors are members of the Cys-loop family of ligand-gated ion channels that are responsible for fast excitatory and inhibitory neurotransmission in the central and peripheral nervous systems. The family includes nicotinic acetylcholine (nACh), GABA, and glycine receptors, all of which are cell-surface, transmembrane proteins. They are composed of five subunits that surround a central ion-conducting pore, and each subunit contains three distinct functional regions that are referred to as the extracellular, transmembrane, and intracellular domains. The orthosteric binding site (which is occupied by the endogenous agonist) is found at the interface of two adjacent extracellular domains and is formed by the convergence of three amino acid loops from one subunit (loops A–C) and three β-sheets (loops D–F) from the other (Thompson et al., 2010; Hassaine et al., 2014). The transmembrane domain contains twenty α-helices, four from each subunit (M1–M4), with M2 from each surrounding the central ion-conducting pore. The intracellular domain is largely unstructured and is responsible for trafficking, intracellular modulation, and ion channel conductance (Peters et al., 2010; Hassaine et al., 2014). The extracellular and transmembrane domains are the main drug targets, with competitive antagonists being of clinical relevance for alleviating the symptoms of nausea and vomiting associated with chemotherapy, radiotherapy, and general anesthesia (Thompson, 2013). There has also been limited use of competitive antagonists in the prevention of irritable bowel syndrome, and the use of partial agonists has been proposed for the same disorder (Moore et al., 2013). Off-target effects at 5-HT_3 receptors have also been described. For the smoking cessation drug varenicline (Champix; Pfizer, Surrey, UK), agonist activity is seen at 5-HT_3 receptors, and it is likely that this is responsible for the most commonly reported side effect, which is nausea. As gastrointestinal side effects, such as abdominal pain, constipation, and vomiting, are also sometimes experienced following the oral administration of proguanil, it is possible that 5-HT_3 receptors are similarly responsible (Wattanagoon et al., 1987). Other antimalarial drugs, such as

This work was funded by the British Heart Foundation [PG/13/39/30293 (to A.J.T.)]; and the Swiss National Science Foundation [SNSF professorship PP00P2_146321/1 (to M.L.)].
dx.doi.org/10.1124/jpet.114.218461.

ABBREVIATIONS: CG, cycloguanil; CPB, 4-chlorophenyl-1-biguanide; HEK, human embryonic kidney; 5-HT, 5-hydroxytryptamine; *m*CPBG, *meta*-chlorophenyl biguanide; nACh, nicotinic acetylcholine.

quinine, chloroquine, and mefloquine (Lariam; Roche, Basel, Switzerland), also have off-target effects at 5-HT$_3$ receptors, as well as at other members of the family. Quinine acts as a competitive antagonist at 5-HT$_3$ receptors, while chloroquine and mefloquine show mixed competitive/noncompetitive antagonist actions (Sieb et al., 1996; Ballestero et al., 2005; Thompson and Lummis, 2008; Lummis et al., 2011).

In this study, we used a combination of electrophysiology, radioligand binding, and in silico ligand docking to provide evidence for the actions of the antimalarial drug proguanil and its metabolites at 5-HT$_3$ receptors.

Materials and Methods

Proguanil was from Sigma-Aldrich (St. Louis, MO), *m*CPBG from Tocris (Bristol, UK), CPB from Fluorochem (Hadfield, UK), and CG from Santa Cruz Biotechnology Inc. (Dallas, TX). Purity was ≥98% for all compounds. In particular, NMR analysis by both the manufacturer and our own facilities showed that CPB was not contaminated with the isomer *m*CPBG. Human 5-HT3A (accession number P46098) subunit cDNA was kindly provided by J. Peters (Dundee University, Dundee, UK).

Oocyte Maintenance. *Xenopus laevis* oocyte–positive females were purchased from Nasco (Fort Atkinson, WI) and maintained according to standard methods. Harvested stage V–VI *Xenopus* oocytes were washed in four changes of ND96 (96 mM NaCl, 2 mM KCl, 1 mM $MgCl_2$, and 5 mM HEPES; pH 7.5); defolliculated in 1.5 mg ml^{-1} collagenase type 1A for 1.5–2 hours; washed again in four changes of ND96; and stored in ND96 containing 2.5 mM sodium pyruvate, 50 mM gentamycin, and 0.7 mM theophylline.

Cell Culture. Human embryonic kidney (HEK) 293T cells were grown on 90-mm round tissue culture plates as monolayers in Dulbecco's modified Eagle's medium/F12 (Gibco/Life Technologies, Carlsbad, CA) supplemented with 10% fetal bovine serum (BioConcept, Allschwil, Switzerland) at 37°C in a moist atmosphere containing 5% CO_2.

Receptor Expression. 5-HT3A subunit cDNA was cloned into pGEMHE for oocyte expression. cRNA was in vitro transcribed from linearized plasmid cDNA template using the mMessage mMachine Ultra T7 Transcription kit (Ambion, Austin, TX). Stage V and VI oocytes were injected with 50 nl of 100–500 ng/μl cRNA (5–25 ng injected), and currents were recorded 1–4 days postinjection.

5-HT3A subunit cDNA was cloned into pcDNA3.1 for expression in HEK293T cells. Cells were transiently transfected with this cDNA using polyethyleneimine (25 kDa, linear, powder; Polysciences Inc., Eppelheim, Germany). Thirty microliters of polyethyleneimine (1 mg ml^{-1}), 5 μl of cDNA, and 1 ml of Dulbecco's modified Eagle's medium were incubated for 10 minutes at room temperature, added dropwise to a 90-mm plate of 80%–90% confluent HEK293T cells, and incubated for 2–3 days before harvesting.

Electrophysiology. Using a two-electrode voltage clamp, *Xenopus* oocytes were routinely clamped at −60 mV using an OC-725 amplifier (Warner Instruments, Hamden, CT), NI USB-6341 X Series DAQ Device (National Instruments, Newbury, UK), and the Strathclyde Electrophysiology Software package v4.7.3 (University of Strathclyde, Glasgow, UK). Microelectrodes were fabricated from borosilicate glass (GC120TF-10; Harvard Apparatus, Edenbridge, UK) using a two-stage horizontal pull (P-97; Sutter Instrument, Novato, CA) and filled with 3 M KCl. Pipette resistances ranged from 0.8–1.5 MΩ. Oocytes were placed in a perfusion chamber made from 2 mm wide × 30 mm long silicon tubing that was cut in half lengthways (total volume, ~0.1 ml) and were perfused with ND96 at a rate of 15 ml min^{-1}. Drug application was via a simple gravity-fed system calibrated to run at the same rate.

Radioligand Binding. Saturation binding (8-point) curves were measured by incubating crude extracts of HEK293T cells stably expressing 5-HT$_3$ receptors in 0.5 ml of HEPES buffer (pH 7.4) containing 0.1–20 nM [^{3}H]granisetron. Competition binding (10-point) was determined by incubating the same cell extracts in 0.5 ml of HEPES buffer (pH 7.4) containing 0.6 nM [^{3}H]granisetron and differing concentrations of competing ligands. Nonspecific binding was determined with 1 mM quipazine or 10 μM tropisetron, which gave similar results. Incubations were terminated by filtration onto Whatman GF/B filters (Sigma-Aldrich) and radioactivity measured using a Tri-Carb 2100TR (PerkinElmer, Waltham, MA) scintillation counter.

Data Analysis. All data analysis was performed with GraphPad Prism v5.00 (GraphPad Software, Inc., La Jolla, CA). The peak current was measured for a range of concentrations and normalized to the maximum peak current for the same oocyte. For inhibition curves, antagonists were routinely coapplied in the presence of 2 μM 5-HT or continuously applied for 1 minute before the coapplication of 2 μM 5-HT. A 2-minute wash was used between drug applications. The mean and S.E.M. for a series of oocytes was plotted against agonist or antagonist concentration and iteratively fitted to the following equation:

$$y = I_{min} + \frac{I_{max} - I_{min}}{1 + 10^{\log(EC_{50} - x)n_H}} \quad (1)$$

where I_{min} is the baseline current, I_{max} is the peak current evoked by agonist, EC_{50} is the concentration of agonist needed to evoke a half-maximal response, x is the ligand concentration, and n_H is the Hill slope. K_b was estimated from IC_{50} values using the Cheng-Prusoff equation with the modification by Leff and Dougall (1993):

$$K_b = \frac{IC_{50}}{\left(\left(2 + \left([A]/[A_{50}]\right)^{n_H}\right)^{1/n_H}\right) - 1} \quad (2)$$

where K_b is the dissociation constant of the competing drug, IC_{50} is the concentration of antagonist required to half the maximal response, $[A]$ is the agonist concentration, $[A_{50}]$ is the agonist EC_{50}, and n_H is the Hill slope of the agonist.

Analysis of competitive inhibition was performed by Schild plot according to the following equation:

$$\log\left[(EC_{50}'/EC_{50}) - 1\right] = \log[L] - \log K_b \quad (3)$$

where EC_{50}' and EC_{50} are values in the presence and absence of antagonist (dose ratio), $[L]$ is the concentration of antagonist, and K_b is the equilibrium dissociation constant for the antagonist-receptor interaction. Further analysis was performed using the Gaddum-Schild equation (slope = 1) as recommended by Neubig et al. (2003) and Lew and Angus (1995):

$$pEC_{50} = -\log\left([L] + 10^{-pA_2}\right) - \log C \quad (4)$$

where pEC_{50} is the negative logarithm of the agonist EC_{50}, $[L]$ is the antagonist concentration, $\log C$ is a constant, and pA_2 is the negative logarithm of the antagonist concentration needed to double the concentration of agonist required to elicit a response that is comparable to the original response in the absence of antagonist. pA_2 is equal to the negative logarithm of K_b when the slope of the Schild plot is exactly 1.

Kinetic parameters were determined according to the following model of a simple bimolecular binding scheme:

$$L + R \underset{k_{off}}{\overset{k_{on}}{\rightleftharpoons}} LR \quad (5)$$

where L is the free ligand concentration, R is receptor concentration, LR is the ligand-receptor complex, and k_{on} and k_{off} are the microscopic association and dissociation rate constants. In a simple scheme such as this, the equilibrium dissociation constant (K_d) is equal to the ratio of dissociation to association rate constants, such that:

$$K_b = \frac{k_{-1}}{k_{+1}} \quad (6)$$

According to a one-site binding model of the type shown, the rates of onset and recovery of an antagonist response can be used to estimate k_{+1} and k_{-1}:

$$1/\tau_{off} = k_{-1} \quad (7)$$

and

$$1/\tau_{on} = k_{+1}[L] + k_{-1} \quad (8)$$

where τ_{on} refers to the rate of onset of inhibition, τ_{off} refers to recovery from inhibition, and $[L]$ is antagonist concentration.

Radioligand saturation binding experiments were analyzed by iterative curve fitting according to:

$$y = \frac{A_{max} \cdot [L]}{K_d + [L]} \quad (9)$$

where y is bound ligand, A_{max} is the maximum signal at equilibrium, K_d is the equilibrium dissociation constant, and $[L]$ is the free concentration of labeled ligand.

Radioligand competition binding data were analyzed by iterative curve fitting according to:

$$y = A_{min} \frac{A_{max} - A_{min}}{1 + 10^{[L] - \log IC_{50}}} \quad (10)$$

where A_{min} is the minimum signal, A_{max} is the maximum signal, $[L]$ is the concentration of competing ligand, and IC_{50} the concentration of competing ligand that blocks half the signal.

K_i values were determined from the IC_{50} values using the Cheng-Prusoff equation:

$$K_i = \frac{IC_{50}}{1 + [L]/K_d} \quad (11)$$

where K_i is the equilibrium dissociation constant for binding of the unlabeled ligand, $[L]$ is the concentration of labeled ligand, and K_d is the equilibrium dissociation constant of the labeled ligand.

Homology Modeling. The protein sequence of the human 5-HT3A subunit (accession number P46098) was aligned with a tropisetron-bound acetylcholine-binding protein template (PDB ID 2WNC) using FUGUE (Shi et al., 2001). With Modeler 9.9, five homology models were generated using default parameters and the best model selected using Ramachandran plot analysis. For the ligand, the protonated forms of proguanil and *m*CPBG were constructed ab initio in Chem3D Ultra 7.0 (CambridgeSoft, Cambridge, UK) and energy-minimized using the included MM2 force field. The binding site was defined as being within 5 Å of the α-carbon of W183, a residue that is centrally located in the binding site and is important for the binding of other 5-HT_3 competitive ligands. The ligands were docked into this site using the GOLD docking program (version 3.0; The Cambridge Crystallographic Data Centre, Cambridge, UK) with the GOLDScore function and default settings. Ten docking poses were generated for each ligand and the poses visualized with PyMol v1.3 (DeLano Scientific LLC, San Francisco, CA).

Results

Effects of Proguanil on 5-HT_3 Receptor Currents. Application of 5-HT or *m*CPBG (Fig. 1) to *Xenopus* oocytes expressing the 5-HT_3 receptor produced concentration-dependent, rapidly activating, inward currents that slowly desensitized over the time course of the applications. Plotting current amplitude against a series of agonist concentrations allowed the data to be fitted with eq. 1. For 5-HT, this gave a pEC_{50} of 5.77 ± 0.04 (EC_{50} = 1.70 μM; n = 9) and Hill slope of 1.68 ± 0.23, and for *m*CPBG a pEC_{50} of 5.45 ± 0.07 (EC_{50} = 3.55 μM; n = 8) and Hill slope of 1.53 ± 0.28 (Fig. 2A). The relative maximal current of *m*CPBG compared with 5-HT was similar (I/I_{max} = 0.94 ± 0.05), consistent with reports elsewhere (Michaelson et al., 2013; Thompson and Lummis, 2013). Agonist responses were completely inhibited by the established 5-HT_3 receptor-specific antagonists granisetron and palonosetron (100 nM; data not shown). Uninjected oocytes did not respond to 5-HT or *m*CPBG.

Application of proguanil alone did not elicit a response, but it caused concentration-dependent inhibition of the 2 μM 5-HT–evoked response (Fig. 2B; Table 1). The pIC_{50} value for proguanil was 5.74 ± 0.06 (IC_{50} = 1.81 μM; n = 8) with a Hill slope of 1.03 ± 0.13. This IC_{50} gave a K_b of 1.74 μM (eq. 2). Inhibition was fully reversible after 1 minute of washing and was unaltered by preapplication (Fig. 2C, upper panel). To test whether proguanil blocked the 5-HT_3 receptor channel, experiments were performed at holding potentials of −40 and +40 mV. The biguanide side chain of proguanil is basic and thus positively charged under physiologic conditions (calculated pK_a values for the imine-type NH groups are 8.2 and 10.4, respectively), so binding in the channel should be influenced by changes in the membrane holding potential. Comparison of proguanil inhibition at −40 and +40 mV revealed

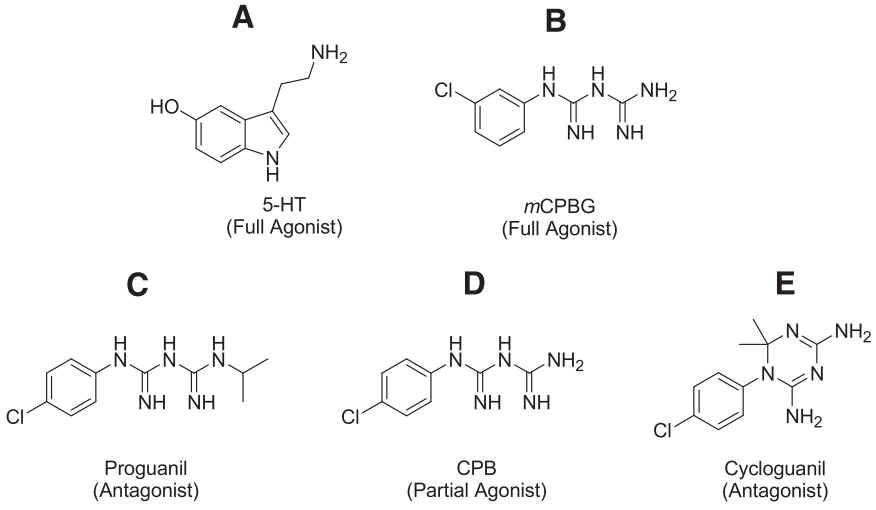

Fig. 1. Chemical structures of the compounds used in this study. 5-HT (A) and *m*CPBG (B) are established 5-HT_3 receptor agonists. Proguanil (C) is an antimalarial prodrug that is converted to CPB (D) and the active metabolite CG (E) by a cytochrome P450–dependent process in the liver.

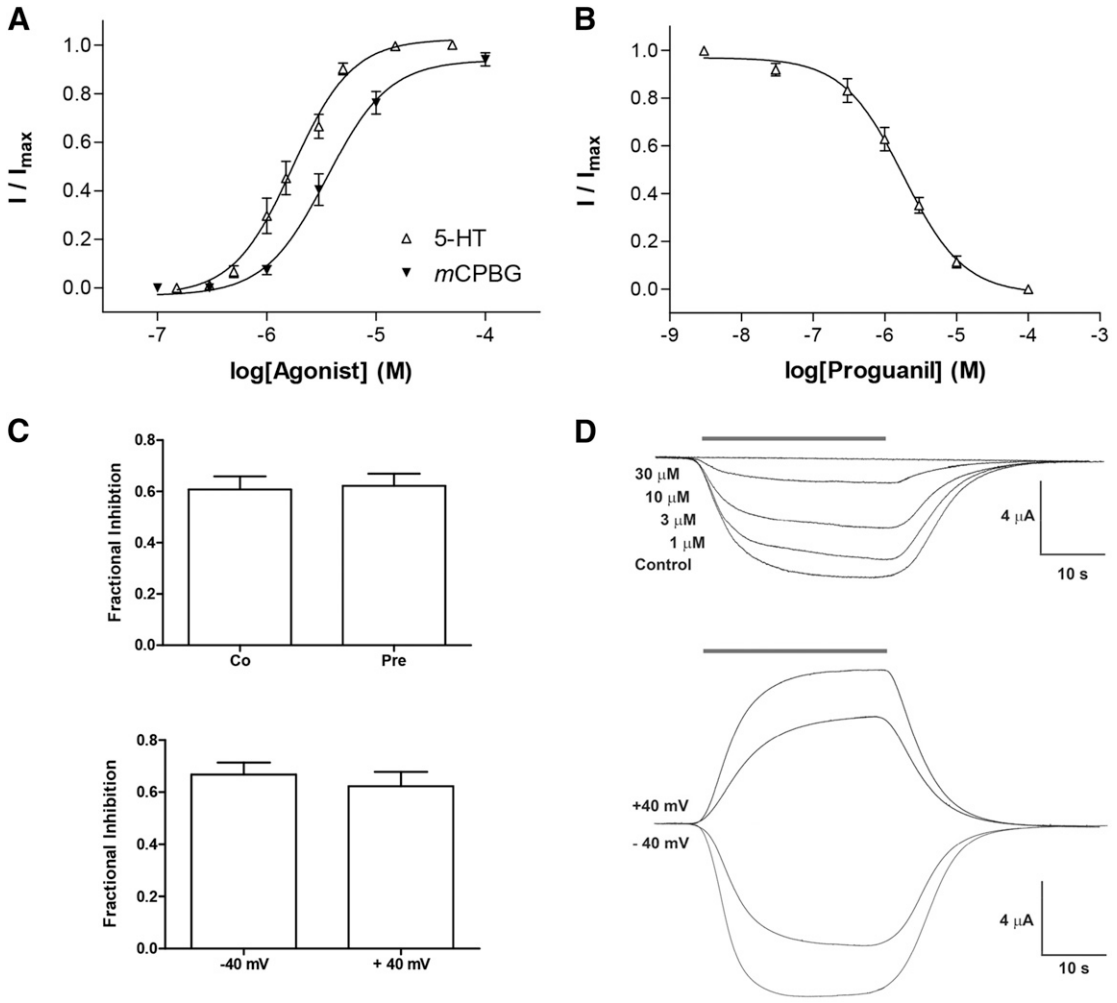

Fig. 2. Agonist properties of 5-HT$_3$ receptors and their inhibition by proguanil. (A) Concentration-response curves for 5-HT and *m*CPBG. (B) Concentration inhibition of the 2 μM 5-HT response by proguanil. (C) Inhibition was unaltered by preapplication of proguanil for 1 minute [$P > 0.05$, paired t test; coapplication (Co) = 0.61 ± 0.05, n = 7; preapplication (Pre) = 0.62 ± 0.05, n = 7] and was not voltage-dependent ($P > 0.05$, paired t test; −40 mV = 0.67 ± 0.04, n = 6; +40 mV = 0.62 ± 0.05, n = 6). (D) The upper panel shows a typical response to 2 μM 5-HT alone and inhibition of the same 5-HT concentration by varying concentrations of proguanil. The lower panel shows typical 2 μM 5-HT responses and their inhibition by 3 μM proguanil at +40 and −40 mV. The gray bar above the traces indicates the application of 5-HT or 5-HT + proguanil. The data in (A) and (B) are normalized to the maximum peak response in each oocyte and represented as the mean ± S.E.M. for a series of oocytes. Parameters derived from these curves can be found in the text and Table 1.

that the levels of inhibition were indistinguishable at these two potentials, showing that proguanil is unlikely to bind in the channel (Fig. 2C, lower panel).

Mechanism of Proguanil Block. Increasing the concentration of proguanil (5, 10, 20, and 40 μM) caused a parallel rightward shift in the 5-HT concentration-response curve, with no change in the maximal response (Fig. 3A; Table 1). A Schild plot of these results (Fig. 3B) yielded a gradient close to 1 (1.08 ± 0.09; R^2 = 0.98) and a pA_2 value of 5.77 ± 0.47 (K_b = 1.70 μM). The K_b was similar (2.87 μM) if the data were fitted using a nonlinear regression method (eq. 4). These data support a competitive mechanism of action, indicating that proguanil binds to the same orthosteric binding site as 5-HT.

A Simple Kinetic Scheme for Proguanil Binding. There are limitations to measuring microscopic rate constants using a two-electrode voltage clamp, but the experiments described in this study were performed under the same conditions, which makes a comparison of relative rates valuable (Papke and Thinschmidt, 1998; Thompson et al., 2007). Inhibition of the 2 μM 5-HT response allowed the microscopic rates of association and dissociation for proguanil to be well fitted by monoexponential functions (Fig. 4; Table 2) that were not significantly affected by the much slower underlying desensitization of the 5-HT current response (τ_{off} = 39 ± 5 seconds; n = 9). When the reciprocal of these rates was plotted against antagonist

TABLE 1
Parameters derived from concentration-response curves in the presence of increasing concentrations of proguanil

Proguanil Concentration	pEC$_{50}$	EC$_{50}$	n_H	n
μM		μM		
0 (control)	5.77 ± 0.04	1.68	1.68	9
5	5.43 ± 0.03	3.71	1.52	5
10	5.30 ± 0.05	5.01	1.22	5
20	4.95 ± 0.05	11.2	1.30	6
40	4.72 ± 0.03	19.0	1.31	4

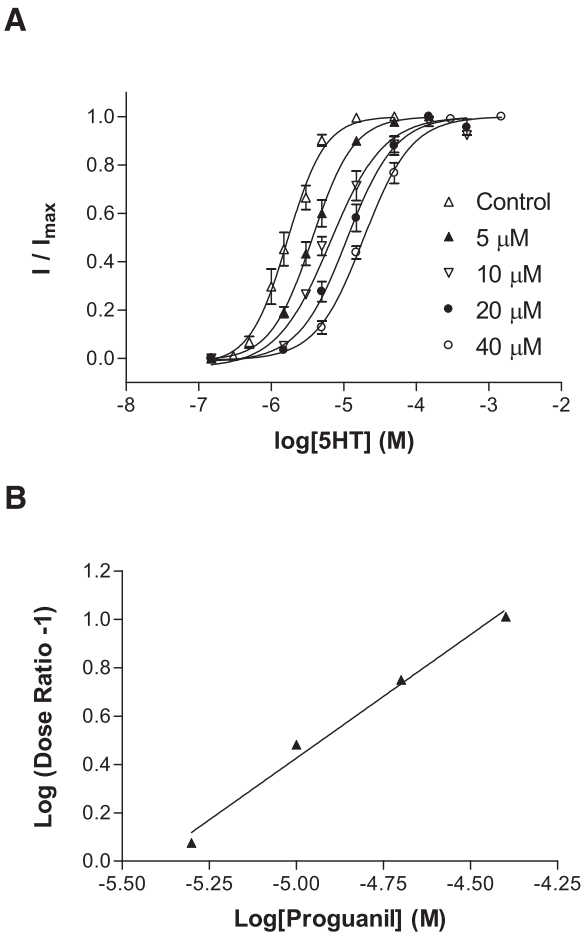

Fig. 3. The mechanism of 5-HT_3 receptor inhibition by proguanil. (A) Concentration-response curves were performed in the absence or presence of the indicated concentrations of proguanil. The curves showed parallel dextral shifts, and maximal currents were restored by increasing concentrations of 5-HT. Parameters derived from these curves can be seen in Table 2. (B) A Schild plot was created from the EC_{50} values of the curves shown in (A) and fitted with eq. 3 to yield a pA_2 of 5.77 ± 0.47 (K_b, 1.70 μM).

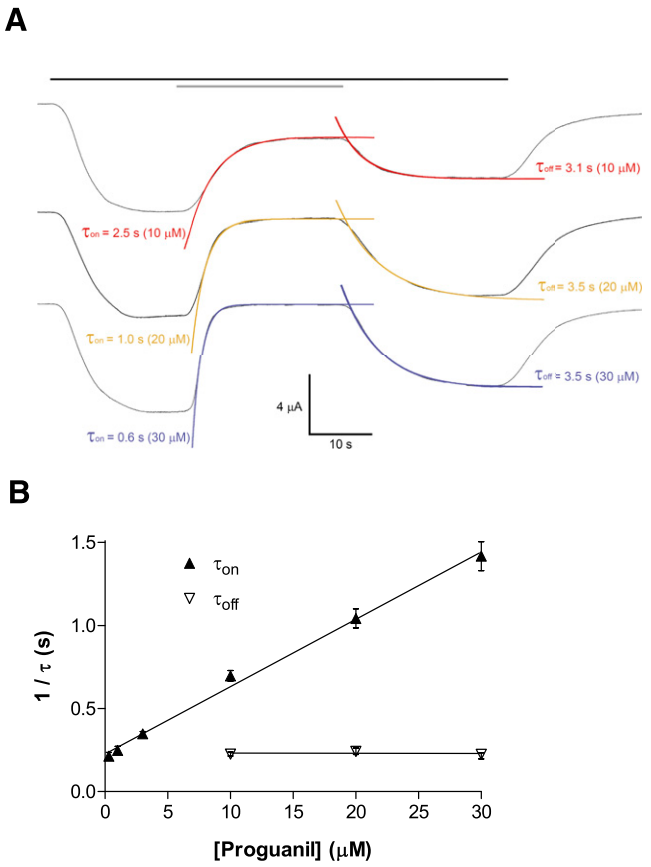

Fig. 4. Kinetics of proguanil interactions at the 5-HT_3 receptor. (A) Sample traces showing the onset (τ_{on}) and recovery (τ_{off}) of proguanil inhibition (gray bar) during a 2 μM 5-HT application (black bar). (B) Association and dissociation constants for inhibition were well fitted by monoexponential functions to give the values shown in Table 2. A plot of the reciprocal of these rates versus the proguanil concentration shows that the association rate (k_{on}) changed linearly with proguanil concentration, while the dissociation rate (k_{off}) did not alter significantly. This is consistent with a simple bimolecular reaction scheme (eqs. 5–8).

concentration, the rates of onset of inhibition (τ_{on}) for proguanil increased linearly with the antagonist concentration, while recovery (τ_{off}) was unaltered, as predicted by eq. 5 (Fig. 4B). The association rate (k_{on}) was determined from the slope of the $1/\tau_{on}$ curve and the dissociation rate constant from the y-axis intercept. The association rate for proguanil was $4.0 \times 10^4\ M^{-1}\ s^{-1}$, and the dissociation rate was $0.23\ s^{-1}$, giving a K_b of 4.35 μM (eq. 6); direct measurements of dissociation gave the same value for k_{off} (Table 2). This analysis is in agreement with a simple kinetic scheme that predicts a single population of binding sites with equal affinities. The affinities were similar to those determined using the other electrophysiologic methods described here and provide further support for a simple competitive mechanism of action.

Competitive Binding with [^{3}H]Granisetron. To further test for a competitive behavior, we measured [^{3}H]granisetron binding in the presence of increasing concentrations of proguanil. Proguanil displayed concentration-dependent competition with 0.6 nM [^{3}H]granisetron (~ K_d; Fig. 5). The average pK_i (eq. 11) of proguanil calculated from a series of separate competition-binding curves was 5.58 ± 0.10 (K_i = 2.61 μM; n = 7). This value is similar to the affinities measured using electrophysiologic methods and provides further support for a competitive mode of action.

Docking Studies. Based on the pharmacologic evidence that proguanil binds at the orthosteric binding site, we used a bioinformatics approach to dock proguanil into a homology model of the 5-HT_3 receptor. Docking of proguanil yielded ligand orientations that fell into four distinct poses that we designated I, II, III, and IV based on the orientation of the ligand and GOLD scores (Olsen et al., 2004). In pose I (Fig. 6A), the phenyl ring of proguanil is located between the aromatic rings of W90, Y153, W183, and Y234, and the biguanide side chain is pointing toward the membrane. There is a potential hydrogen bond between an imine NH group and the backbone carbonyl of W183. In pose II (Fig. 6B), the phenyl ring of proguanil is also located between the aromatic rings of W90, Y153, W183, and Y234, with the isopropyl group of the biguanide making a hydrophobic contact with the aromatic ring of Y143. In addition, the biguanide NH groups can potentially form hydrogen bonds with the hydroxyl group of Y234 on the principal face and the amide group of Q151 on the complementary face. In pose III (Fig. 6C), the biguanide moiety of proguanil is located in the aromatic box formed by

TABLE 2
Rates of inhibition and recovery of 2 μM 5-HT responses in the presence of increasing concentrations of proguanil

Proguanil Concentration	τ_{on}	n	τ_{off}	n
μM	s		s	
0.3	0.21 ± 0.02	9	–	–
1	0.25 ± 0.02	14	–	–
3	0.35 ± 0.01	16	–	–
10	0.70 ± 0.03	14	0.23 ± 0.01	15
20	1.04 ± 0.06	15	0.24 ± 0.02	12
30	1.42 ± 0.09	12	0.21 ± 0.02	12

–, no value measured at this concentration.

the rings of W90, Y153, W183, and Y234, and potential hydrogen bonds are formed between the NH groups of proguanil and the side chains of loop C residues S230 and Y234 and side chains of loop E residues Q151 and Y153. In addition, the phenyl ring of proguanil engages in a hydrophobic interaction with the aromatic ring of Y143. Finally, pose IV (Fig. 6D) places the biguanide moiety in the aromatic box, but the phenyl ring of proguanil is pointing toward loop C. Potential hydrogen bonds are formed between biguanide NH groups and the hydroxyl groups of S230 and Y234 and the backbone carbonyls of S182 and W183.

Proguanil shares many structural similarities with *m*CPBG (Fig. 1), for which there is evidence in the literature to support our docking (see *Discussion*). We therefore also docked *m*CPBG into the 5-HT$_3$ receptor homology model. Contrary to the diversity of predicted binding models for proguanil, all but 1 of the top 10 docking solutions predicted only one binding pose for *m*CPBG (Fig. 6E). In this pose, the phenyl ring of *m*CPBG is located in the center of the aromatic box formed by the rings of W90, Y153, W183, and Y234, and the biguanide side chain is pointing toward the aromatic ring of Y143, potentially forming a cation-π interaction. The average distance between the terminal nitrogen of the biguanide and the aromatic ring carbons of Y143 is approximately 5 Å, which is ideal for this attractive interaction. In addition, potential hydrogen bonds are formed between NH groups of the biguanide moiety and side chains of Q151, S230, and Y234 and the backbone carbonyl of L184. This pose is most similar to pose II for proguanil.

Effects of Proguanil Metabolites on 5-HT$_3$ Receptor Currents. Proguanil is metabolized to CG and CPB by cytochrome P450 enzymes in the liver. To determine whether these two metabolites also influence 5-HT$_3$ receptor currents, their effects on 2 μM 5-HT responses was measured at varying concentrations of each. CG reversibly inhibited these 5-HT responses with a pIC$_{50}$ of 5.83 ± 0.04 (IC$_{50}$ = 1.48 μM; n = 8) and a Hill slope of 1.11 ± 0.15. This yielded a K_b of 1.42 μM, which was similar to that measured for the parent compound proguanil (eq. 2; Fig. 7A). Similar to proguanil, the presence of increasing concentrations of CG also caused parallel dextral shifts in 5-HT concentration-response curves and inhibition was surmountable with increased concentrations of 5-HT (Fig. 7C). An analysis of the changes in the resultant EC$_{50}$ values by Schild plot gave a pA_2 of 5.53 (K_b = 2.95 μM).

CPB reversibly inhibited 2 μM 5-HT responses with a pIC$_{50}$ of 5.36 ± 0.06 (IC$_{50}$ = 4.36 μM; n = 7) and a Hill slope of 1.10 ± 0.16, which yielded a K_b of 4.19 μM (eq. 2). CPB caused similar parallel and surmountable shifts in 5-HT concentration-response curves that gave a pA_2 of 4.94 (K_b = 11.4 μM) when analyzed by Schild plot (Fig. 7D). In addition to these inhibitory effects, at higher concentrations, CPB was also a low-efficacy partial agonist with a pEC$_{50}$ of 4.85 ± 0.12 (EC$_{50}$ = 14.1 μM; n = 6) and a maximal current response relative to 100 μM 5-HT of 0.013 ± 0.001 (Fig. 8).

The effects of both metabolites were fully reversible after 1 minute of washing and were unaltered by preapplication or holding potential (Fig. 7, E and F). The surmountable inhibition, partial agonism, and absence of voltage dependence were consistent with a competitive mechanism of action for both ligands.

Competition of Proguanil Metabolites with [^{3}H]Granisetron. To confirm our electrophysiologic results, CG and CPB were also examined using radioligand competition with 0.6 nM [^{3}H]granisetron. This gave a pK_i value of 5.31 ± 0.11 (K_i = 4.89 μM; n = 6) for CG, which was similar to the affinity calculated by the Cheng-Prusoff equation (eq. 2) or Schild analysis (eq. 3). CPB had a higher affinity than CG, with a pK_i of 6.39 ± 0.07 (K_i = 0.41 μM; n = 5) that was 10- to 27-fold higher than values calculated by the Cheng-Prusoff equation (eq. 2) or Schild analysis (eq. 3). For both ligands, these results are consistent with a competitive mode of action.

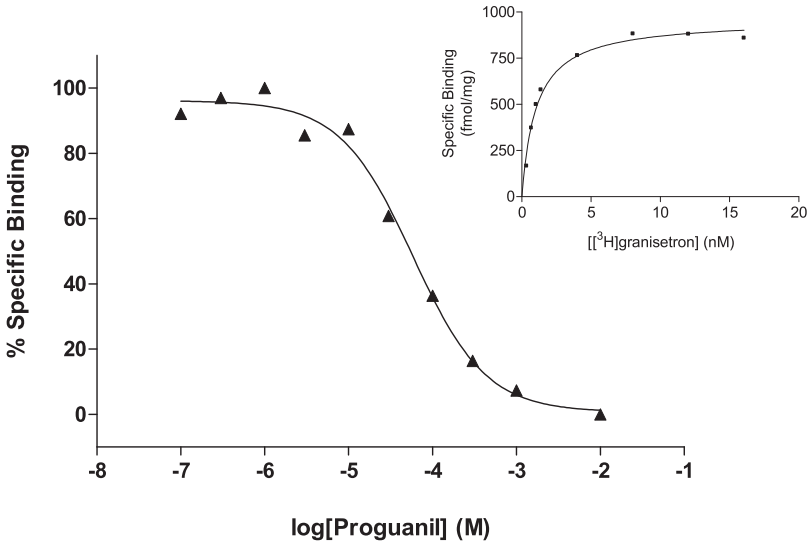

Fig. 5. An example binding curve for the competition of 0.6 nM [^{3}H]granisetron and varying concentrations of proguanil at 5-HT$_3$ receptors from transiently transfected HEK293T cells. The curve is a single experiment that is representative of six additional curves. Data were normalized to [^{3}H]granisetron binding in the absence of antagonist and fitted with eq. 10. Data from each of the separate curves were averaged to give the mean ± S.E.M. shown in the text. (Inset) A typical saturated binding curve for [^{3}H]granisetron alone.

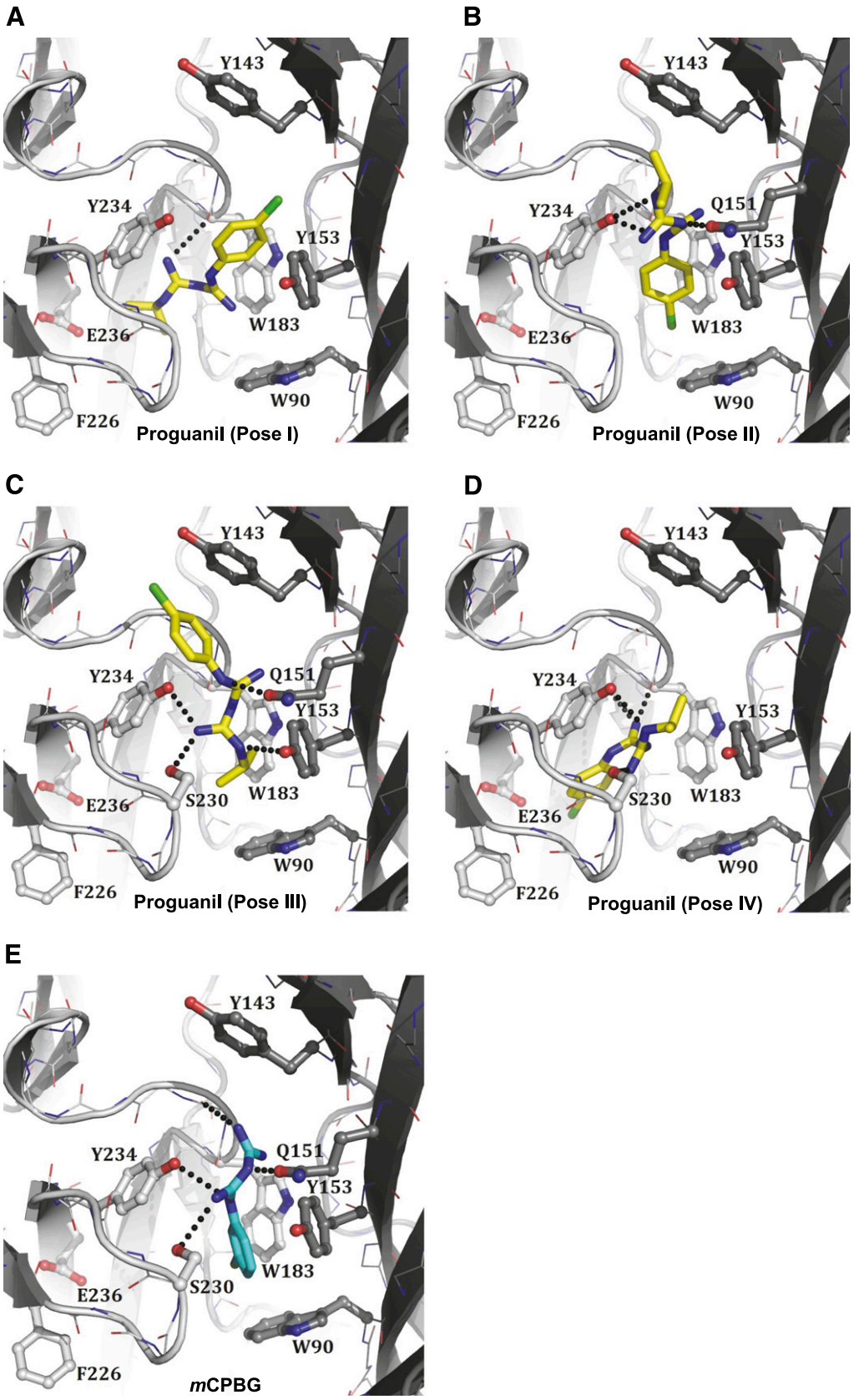

Fig. 6. Representative examples of docked ligands in the 5-HT_3 receptor orthosteric binding site, showing the orientation of the main residues that define these models. Proposed binding poses for proguanil (yellow, A–D) and *m*CPBG (blue, E) are shown. The principal face (left, light gray), complementary face (right, dark gray), peptide backbone (line representation), and side chains (ball-and-stick representation) of residues discussed in the text are highlighted. Dotted lines indicate potential hydrogen bonds and are described in the text.

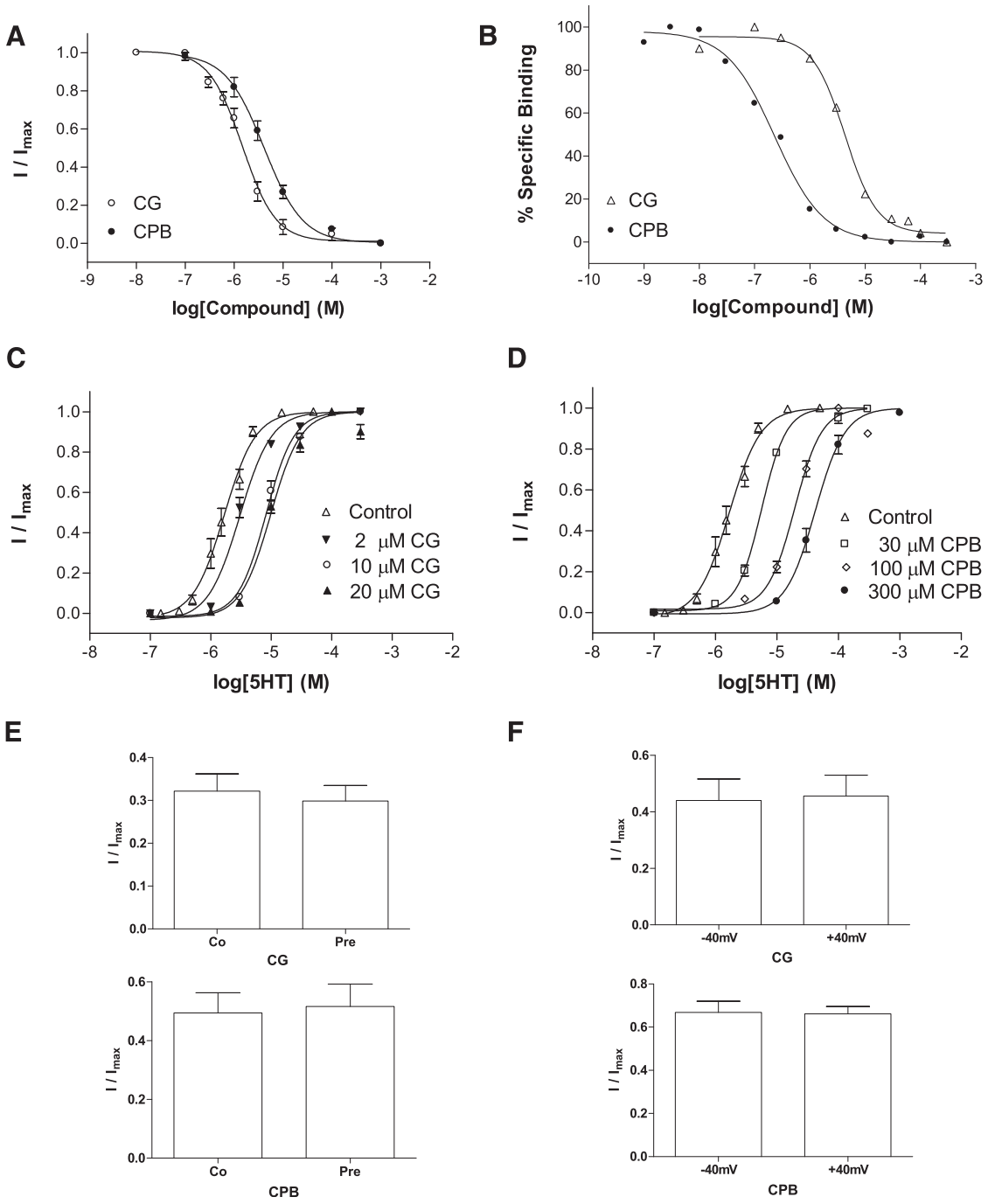

Fig. 7. Properties of CG and CPB on 5-HT$_3$ receptors. (A) Both CG and CPB inhibited the 2 μM 5-HT response in a concentration-dependent manner. (B) Representative experiments of competition binding between 0.6 nM [^{3}H]granisetron and increasing concentrations of CG and CPB; pIC$_{50}$ values calculated (eq. 10) from these single curves were averaged with similar values from additional experiments and are shown as mean ± S.E.M. in the text. (C) 5-HT concentration-response curves were performed in the absence or presence of increasing concentrations of CG and showed parallel dextral shifts that were surmountable at higher concentrations of 5-HT. (D) Increasing concentrations of CPB had similar effects as those shown in (C). (E) The levels of inhibition caused by 3 μM CG or 3 μM CPB were not altered when the compounds were coapplied (Co) with 2 μM 5-HT or preapplied (Pre) for 1 minute followed by immediate coapplication ($P > 0.05$, paired t test; CG, Co = 0.28 ± 0.02, $n = 5$; Pre = 0.26 ± 0.01, $n = 5$; CPB, Co = 0.49 ± 0.07, $n = 6$; Pre = 0.51 ± 0.08, $n = 4$). (F) Inhibition by CG and CPB did not differ at −40 and +40 mV ($P > 0.05$, paired t test; CG, −40 mV = 0.45 ± 0.07, $n = 5$; +40 mV = 0.44 ± 0.07, $n = 5$; CPB, −40 mV = 0.69 ± 0.05, $n = 5$; +40 mV = 0.66 ± 0.03, $n = 6$). IC$_{50}$ values and Hill slopes derived from the curves can be found in the text.

Discussion

This study describes the effects of the antimalarial compound proguanil and its metabolites, CG and CPB, on human 5-HT$_3$ receptors. All were relatively potent inhibitors of 5-HT-mediated currents, with IC$_{50}$ values in the low micromolar range. Competition was shown by surmountable rightward shifts of 5-HT concentration-response curves in the presence of increasing concentrations of the compounds and competition with the radiolabeled antagonist [^{3}H]granisetron. For CPB, a low-efficacy partial agonism was also seen at higher concentrations.

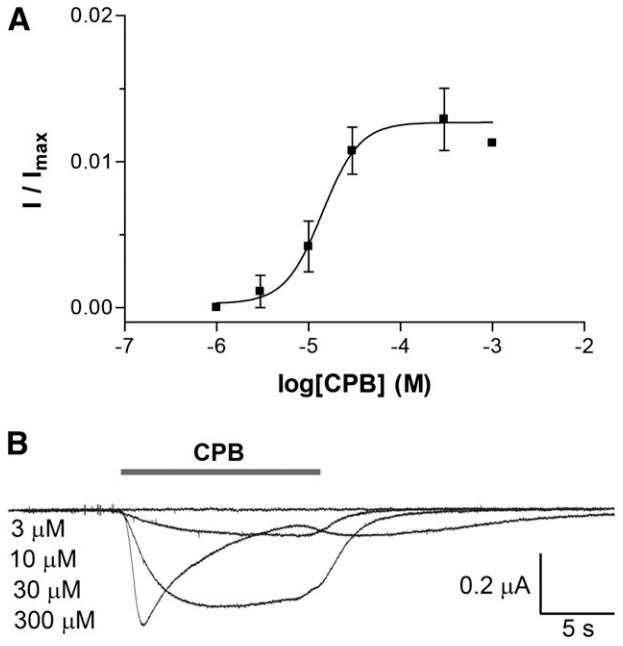

Fig. 8. Agonist properties of CPB. (A) A concentration-response curve for CPB compared with the maximal (100 μM) 5-HT response. CPB was a partial agonist with a lower potency than 5-HT (EC_{50} = 14.1 μM; I/I_{max} = 0.013 ± 0.001; n = 6). A similar dual-action agonist-antagonist action underpins the therapeutic effects of varenicline that relies on the response of the partial agonist suppressing the response of the native ligand to enforce a reduced, but controlled, activation. (B) Example traces for the indicated concentrations of CPB are shown. At >300 μM CPB, the current returns to baseline more rapidly than at lower concentrations. For *m*CPBG, this effect has been studied in detail and is believed to represent autoinhibition of the receptor by agonist channel block at high concentrations (Hapfelmeier et al., 2003). NMR analysis showed that there was no contamination of CPB with the isomer *m*CPBG and the agonist response was therefore an effect of CPB alone.

Proguanil is used as an antimalarial drug in both monotherapy (e.g., Paludrine; AstraZeneca, London, UK) or in combination with other antimalarial compounds (e.g., Malarone; GlaxoSmithKline, Brentford, UK). Against *Plasmodium falciparum* it is considered to be a safe and reliable drug and can be useful in special circumstances, such as in children, pregnant women, and regions of chloroquine resistance (Bradley, 1993; Wangboonskul et al., 1993). Following oral administration of Paludrine (two 100-mg tablets), the whole-blood concentrations of proguanil peak at 4.1 μM after 2–4 hours. For the metabolites CPB and CG, whole-blood concentrations peak at 0.3 μM within the same time frame (Wattanagoon et al., 1987; Wangboonskul et al., 1993). 5-HT_3 receptors are highly expressed in the gut, where they regulate motility, and are responsible for the vomiting reflex that occurs following the stimulation of gastrointestinal vagal afferent nerves. Effects on these receptors may therefore be at least partially responsible for side effects such as abdominal pain, constipation, and vomiting that are sometimes experienced after administration of proguanil (Wattanagoon et al., 1987). Gastrointestinal side effects are also reported for the antimalarials quinine, chloroquine, and mefloquine. These similarly inhibit 5-HT_3 receptors, with IC_{50} values close to plasma concentrations, and antagonize 5-HT_3 receptor–mediated gut contractions (Thompson and Lummis, 2008; Kelley et al., 2014). Strategies to find analogous drugs (e.g., phenoxypropoxybiguanides) may therefore wish to consider their effects on 5-HT_3 receptors as an indication of gut intolerance earlier in their development (Shearer et al., 2005; Zucca et al., 2013). It is also noteworthy that the first-line antidiabetic drug metformin (Bolamyn, Glucophage) is also a biguanide, as are the related antidiabetics phenformin and buformin. Gastrointestinal disturbances are reported for all of these drugs and are the main reason (~30%) for compliance issues in patients taking metformin (Pernicova and Korbonits, 2014). Metformin-evoked release of 5-HT is partially responsible, but gut concentrations of metformin can be close to the 2 mM IC_{50} (pK_i = 2.71 ± 0.05; n = 5) (unpublished data) for this compound and may also have effects (Wilcock and Bailey, 1994).

The observation that proguanil competitively inhibits 5-HT_3 receptor responses was anticipated, as there are structural similarities with the 5-HT_3 receptor agonist *m*CPBG. Indeed, previous structure-activity studies on arylbiguanides have reported the same affinities for CPB as our own, but did not explore agonist activities (Dukat et al., 1996; Glennon et al., 2003). In these studies, an important role for the 3-position substituent was reported, consistent with the importance of the 3-hydroxyl in the agonists 5-HT, dopamine, *m*-tyramine, and *m*CPBG (Meiboom et al., 2013; Thompson and Lummis, 2013). In our own study, the transfer of Cl from the 3- (*m*CPBG) to the 4-position (CPB) caused a dramatic change in agonist efficacy, consistent with these earlier reports. A molecule similar to proguanil, with a terminal *N,N*-dimethyl group, and a 3-Cl rather than the 4-Cl found in proguanil, is reported to have an affinity of >10 μM (Dukat et al., 1996). In contrast, *m*CPBG, which also contains a 3-Cl but has an unsubstituted terminal amine rather than *N,N*-dimethyl, has an affinity in the low- to mid-nanomolar range (Dukat et al., 1996; Hope et al., 1996). This suggests that the unsubstituted terminal amine is more optimal for high-affinity binding than *N,N*-dimethyl, possibly due to reduced steric hindrance and its ability to act as a hydrogen bond donor; *m*CPBG may also have a slightly higher apparent affinity than proguanil because of the influence of gating efficacy on the apparent affinity of agonists (Colquhoun, 1998; Purohit and Grosman, 2006). Truncation of the biguanide chain to the shorter guanidine group, such as in *meta*-chlorophenylguanidine, does not affect affinity or agonist activity (Dukat et al., 2007), but further removal or replacement of one of the two nitrogen atoms in the truncated guanidine moiety abolishes agonist properties, showing that both the aromatic substituent and the nitrogen-containing basic groups are needed for activation (Glennon et al., 2003).

The ligand-receptor interactions that are responsible for *m*CPBG binding have been examined in detail and may be similar for the structurally related compound proguanil. To explore this possibility, we docked proguanil and *m*CPBG into the 5-HT_3 receptor ligand-binding site. The docked pose clusters of both ligands were all located within 5 Å of residues Y143, Y153 (loop E), W183 (loop B), F226, and Y234 (loop C), that form the "aromatic box" that is an established component of the 5-HT_3 receptor-binding site and influence *m*CPBG binding when mutated. In a comprehensive Ala scan of loop E, only residues Y143 and Y153 affected *m*CPBG binding, suggesting specific interactions that are supported by the orientations of *m*CPBG (Fig. 6E) and proguanil poses I–III (Fig. 6, A–C) in our models (Venkataraman et al., 2002). Differences between the actions of *m*CPBG in rodent and human receptors have been entirely attributed to residues in loop C with important contributions made by F226 and Y234

(Mochizuki et al., 1999; Suryanarayanan et al., 2005). In our docked poses, the formation of a hydrogen bond between NH groups of the biguanide moiety and the hydroxyl group and these residues was predicted for both *m*CPBG (Fig. 6E) and proguanil poses II–IV (Fig. 6, B–D). In all of our docked poses, interactions with the loop B residue W183 were also predicted. Loop B forms a major structural component of the orthosteric binding site, and mutations are poorly tolerated throughout the loop (Thompson et al., 2008). In particular, Michaelson et al. (2013) and Spier and Lummis (2000) reported that W183 was important for *m*CPBG binding and activation, and a direct ligand-receptor interaction is likely, as the residue is centrally located in the binding site and mutations affect a wide range of agonists and antagonists without altering receptor expression (Spier and Lummis, 2000; Thompson et al., 2010; Nys et al., 2013). Importantly, none of the poses extended toward loops A or F, both of which are unlikely to interact with proguanil or *m*CPBG; loop F mutations have no effect on *m*CPBG, and evidence from experiments on E129 supports a structural rather than a binding role, as 1) H-bonding is seen between loops A and B in 5-HTBP and 5-HT$_3$ receptor crystal structures, and only H-bonding substitutions produce functional receptors; 2) E129 substitutions cause reduced cell-surface expression; and 3) effects of E129 mutations are the same regardless of the ligands studied (Jensen et al., 2006; Price et al., 2008; Kesters et al., 2013; Hassaine et al., 2014).

Of the four predicted poses for proguanil, we therefore favor pose II (Fig. 6B), which is the most similar to the main docked pose for *m*CPBG. In this pose, the biguanide NH groups form hydrogen bonds with the side chains of Y234 and Q151; the phenyl ring of proguanil can establish hydrophobic interactions with the aromatic rings of W90, Y153, and W183; and the isopropyl end group of the biguanide is in hydrophobic contact with the aromatic ring of Y143. However, in contrast to *m*CPBG, proguanil acts as an antagonist, and yet it is predicted to occupy a similar position. We therefore speculate that proguanil is similarly located, but does not activate the receptor because it lacks the essential 3-Cl and terminal free amine moieties. This may be because proguanil does not have the capability to H-bond that the terminal unsubstituted NH_2 group has, nor the 3-substituent that is known to be necessary for receptor activation (Dukat et al., 2007). In previous studies, direct ligand-receptor interactions and those mediated via a water molecule have been seen between 5-HTBP and 5-HT, and both the size and electronegativity of ligand substituents have been proposed to subtly limit the efficiency of conformational transitions that mediate channel opening (Kesters et al., 2013). With our static models, such interactions are difficult to predict, but given the structural similarities between proguanil and *m*CPBG, and the effects of amino acid substitutions on the binding of the latter, we believe that pose II is broadly representative (Fig. 6B).

Proguanil, CG, and CPB behaved competitively, similar to the actions of the antimalarials quinine and chloroquine at 5-HT$_3$, GABA$_A$, and nACh receptors (Ballestero et al., 2005; Thompson et al., 2007; Thompson and Lummis, 2008). At $\alpha9\alpha10$ nACh and muscle-type acetylcholine receptors, quinine and chloroquine also have additional noncompetitive actions, while the antimalarial mefloquine (Lariam) is largely noncompetitive at low concentrations, but displaces [^{3}H]granisetron at higher concentrations (Sieb et al., 1996; Ballestero et al., 2005; Thompson et al., 2007). Given that proguanil has been reported to affect acetylcholine responses in the cardiovascular system of dogs, it is possible that it also affects nACh receptors and that these antimalarials share conserved modes and sites of action throughout the Cys-loop family (Jindal, 1956).

In summary, we provide the first reported evidence that the antimalarial drug proguanil and its metabolites inhibit the function of homomeric 5-HT$_3$ receptors via competition. This work extends the number of antimalarials that are known to affect different members of the Cys-loop family and, because the concentration of proguanil in the blood exceeds that which inhibits 5-HT$_3$ receptors, may provide a reason for the occasional gastrointestinal side effects experienced by patients consuming these biguanide drugs. Given that the development of related compounds has been previously discontinued as a result of unwanted nausea and vomiting, we suggest an early assessment of promising leads on 5-HT$_3$ receptors.

Acknowledgments

The authors thank John Peters (University of Dundee) for the 5-HT3A subunit and Ruth Murrell-Lagnado for hosting the experimental work.

Authorship Contributions

Participated in research design: Thompson.
Conducted experiments: Thompson.
Performed data analysis: Thompson, Lochner.
Wrote or contributed to the writing of the manuscript: Thompson, Lochner.

References

Ballestero JA, Plazas PV, Kracun S, Gómez-Casati ME, Taranda J, Rothlin CV, Katz E, Millar NS, and Elgoyhen AB (2005) Effects of quinine, quinidine, and chloroquine on $\alpha9\alpha10$ nicotinic cholinergic receptors. *Mol Pharmacol* **68**:822–829.
Bradley D; Malaria Reference Laboratory and the Ross Institute (1993) Prophylaxis against malaria for travellers from the United Kingdom. *BMJ* **306**:1247–1252.
Colquhoun D (1998) Binding, gating, affinity and efficacy: the interpretation of structure-activity relationships for agonists and of the effects of mutating receptors. *Br J Pharmacol* **125**:924–947.
Dukat M, Abdel-Rahman AA, Ismaiel AM, Ingher S, Teitler M, Gyermek L, and Glennon RA (1996) Structure-activity relationships for the binding of arylpiperazines and arylbiguanides at 5-HT3 serotonin receptors. *J Med Chem* **39**: 4017–4026.
Dukat M, Glennon RA, and Young S (2007) MD-354: what is it good for? *CNS Drug Rev* **13**:1–20.
Glennon RA, Daoud MK, Dukat M, Teitler M, Herrick-Davis K, Purohit A, and Syed H (2003) Arylguanidine and arylbiguanide binding at 5-HT3 serotonin receptors: a QSAR study. *Bioorg Med Chem* **11**:4449–4454.
Hassaine G, Deluz C, Grasso L, Wyss R, Tol MB, Hovius R, Graff A, Stahlberg H, Tomizaki T, and Desmyter A, et al. (2014) X-ray structure of the mouse serotonin 5-HT3 receptor. *Nature* **512**:276–281.
Hapfelmeier G, Tredt C, Haseneder R, Zieglgänsberger W, Eisensamer B, Rupprecht R, and Rammes G (2003) Co-expression of the 5-HT3B serotonin receptor subunit alters the biophysics of the 5-HT3 receptor. *Biophys J* **84**:1720–1733.
Hope AG, Peters JA, Brown AM, Lambert JJ, and Blackburn TP (1996) Characterization of a human 5-hydroxytryptamine3 receptor type A (h5-HT3R-AS) subunit stably expressed in HEK 293 cells. *Br J Pharmacol* **118**:1237–1245.
Jensen TN, Nielsen J, Frederiksen K, and Ebert B (2006) Molecular cloning and pharmacological characterization of serotonin 5-HT(3A) receptor subtype in dog. *Eur J Pharmacol* **538**:23–31.
Jindal MN (1956) Effects of quinine, proguanil and chloroquine on cardio-vascular responses of adrenaline and acetylcholine in dogs. *Indian J Med Res* **44**:649–655.
Kelley SP, Walsh J, Kelly MC, Muhdar S, Adel-Aziz M, Barrett ID, and Wildman SS (2014) Inhibition of native 5-HT3 receptor-evoked contractions in guinea pig and mouse ileum by antimalarial drugs. *Eur J Pharmacol* **738**:186–191.
Kesters D, Thompson AJ, Brams M, van Elk R, Spurny R, Geitmann M, Villalgordo JM, Guskov A, Danielson UH, and Lummis SC, et al. (2013) Structural basis of ligand recognition in 5-HT3 receptors. *EMBO Rep* **14**:49–56.
Leff P and Dougall IG (1993) Further concerns over Cheng-Prusoff analysis. *Trends Pharmacol Sci* **14**:110–112.
Lew MJ and Angus JA (1995) Analysis of competitive agonist-antagonist interactions by nonlinear regression. *Trends Pharmacol Sci* **16**:328–337.
Lummis SC, Thompson AJ, Bencherif M, and Lester HA (2011) Varenicline is a potent agonist of the human 5-hydroxytryptamine3 receptor. *J Pharmacol Exp Ther* **339**:125–131.
Meiboom MF, Barann M, Witten S, Groeneveld K, and Urban BW (2013) Which agonist properties are important for the activation of 5-HT3A receptors? *Biochim Biophys Acta* **1828**:2564–2573.

Michaelson SD, Paulsen IM, Kozuska JL, Martin IL, and Dunn SM (2013) Importance of recognition loops B and D in the activation of human 5-HT_3 receptors by 5-HT and meta-chlorophenylbiguanide. *Neuropharmacology* **73**:398–403.
Mochizuki S, Miyake A, and Furuichi K (1999) Identification of a domain affecting agonist potency of meta-chlorophenylbiguanide in 5-HT3 receptors. *Eur J Pharmacol* **369**:125–132.
Moore NA, Sargent BJ, Manning DD, and Guzzo PR (2013) Partial agonism of 5-HT3 receptors: a novel approach to the symptomatic treatment of IBS-D. *ACS Chem Neurosci* **4**:43–47.
Neubig RR, Spedding M, Kenakin T, and Christopoulos A; International Union of Pharmacology Committee on Receptor Nomenclature and Drug Classification (2003) International Union of Pharmacology Committee on Receptor Nomenclature and Drug Classification. XXXVIII. Update on terms and symbols in quantitative pharmacology. *Pharmacol Rev* **55**:597–606.
Nys M, Kesters D, and Ulens C (2013) Structural insights into Cys-loop receptor function and ligand recognition. *Biochem Pharmacol* **86**:1042–1053.
Olsen L, Pettersson I, Hemmingsen L, Adolph HW, and Jørgensen FS (2004) Docking and scoring of metallo-beta-lactamases inhibitors. *J Comput Aided Mol Des* **18**:287–302.
Papke RL and Thinschmidt JS (1998) The correction of α7 nicotinic acetylcholine receptor concentration-response relationships in *Xenopus* oocytes. *Neurosci Lett* **256**:163–166.
Pernicova I and Korbonits M (2014) Metformin—mode of action and clinical implications for diabetes and cancer. *Nat Rev Endocrinol* **10**:143–156.
Peters JA, Cooper MA, Carland JE, Livesey MR, Hales TG, and Lambert JJ (2010) Novel structural determinants of single channel conductance and ion selectivity in 5-hydroxytryptamine type 3 and nicotinic acetylcholine receptors. *J Physiol* **588**: 587–596.
Price KL, Bower KS, Thompson AJ, Lester HA, Dougherty DA, and Lummis SC (2008) A hydrogen bond in loop A is critical for the binding and function of the 5-HT3 receptor. *Biochemistry* **47**:6370–6377.
Purohit Y and Grosman C (2006) Estimating binding affinities of the nicotinic receptor for low-efficacy ligands using mixtures of agonists and two-dimensional concentration-response relationships. *J Gen Physiol* **127**:719–735.
Shearer TW, Kozar MP, O'Neil MT, Smith PL, Schiehser GA, Jacobus DP, Diaz DS, Yang YS, Milhous WK, and Skillman DR (2005) In vitro metabolism of phenoxypropoxybiguanide analogues in human liver microsomes to potent antimalarial dihydrotriazines. *J Med Chem* **48**:2805–2813.
Shi J, Blundell TL, and Mizuguchi K (2001) FUGUE: sequence-structure homology recognition using environment-specific substitution tables and structure- dependent gap penalties. *J Mol Biol* **310**:243–257.
Sieb JP, Milone M, and Engel AG (1996) Effects of the quinoline derivatives quinine, quinidine, and chloroquine on neuromuscular transmission. *Brain Res* **712**:179–189.
Spier AD and Lummis SC (2000) The role of tryptophan residues in the 5-hydroxytryptamine(3) receptor ligand binding domain. *J Biol Chem* **275**:5620–5625.
Suryanarayanan A, Joshi PR, Bikádi Z, Mani M, Kulkarni TR, Gaines C, and Schulte MK (2005) The loop C region of the murine 5-HT3A receptor contributes to the differential actions of 5-hydroxytryptamine and m-chlorophenylbiguanide. *Biochemistry* **44**:9140–9149.
Thompson AJ (2013) Recent developments in 5-HT3 receptor pharmacology. *Trends Pharmacol Sci* **34**:100–109.
Thompson AJ, Lester HA, and Lummis SC (2010) The structural basis of function in Cys-loop receptors. *Q Rev Biophys* **43**:449–499.
Thompson AJ, Lochner M, and Lummis SC (2007) The antimalarial drugs quinine, chloroquine and mefloquine are antagonists at 5-HT3 receptors. *Br J Pharmacol* **151**:666–677.
Thompson AJ, Lochner M, and Lummis SC (2008) Loop B is a major structural component of the 5-HT3 receptor. *Biophys J* **95**:5728–5736.
Thompson AJ and Lummis SC (2008) Antimalarial drugs inhibit human 5-HT(3) and GABA(A) but not GABA(C) receptors. *Br J Pharmacol* **153**:1686–1696.
Thompson AJ and Lummis SC (2013) A single channel mutation alters agonist efficacy at 5-HT3A and 5-HT3AB receptors. *Br J Pharmacol* **170**:391–402.
Venkataraman P, Venkatachalan SP, Joshi PR, Muthalagi M, and Schulte MK (2002) Identification of critical residues in loop E in the 5-HT3ASR binding site. *BMC Biochem* **3**:15.
Wangboonskul J, White NJ, Nosten F, ter Kuile F, Moody RR, and Taylor RB (1993) Single dose pharmacokinetics of proguanil and its metabolites in pregnancy. *Eur J Clin Pharmacol* **44**:247–251.
Wattanagoon Y, Taylor RB, Moody RR, Ochekpe NA, Looareesuwan S, and White NJ (1987) Single dose pharmacokinetics of proguanil and its metabolites in healthy subjects. *Br J Clin Pharmacol* **24**:775–780.
Wilcock C and Bailey CJ (1994) Accumulation of metformin by tissues of the normal and diabetic mouse. *Xenobiotica* **24**:49–57.
Zucca M, Scutera S, and Savoia D (2013) New chemotherapeutic strategies against malaria, leishmaniasis and trypanosomiases. *Curr Med Chem* **20**:502–526.

Address correspondence to: Dr. Andrew J. Thompson, Department of Pharmacology, Cambridge University, Tennis Court Road, Cambridge CB2 1PD, United Kingdom. E-mail: ajt44@cam.ac.uk